

Contribution of remote sensing to the alluvial aquifer's characterization. Case of the Tabarka aquifer (Northwestern Tunisia)

*Contribution de la télédétection à la caractérisation de l'aquifère alluvial.
Cas de l'aquifère de Tabarka (nord-ouest de la Tunisie)*

Gannouni SONIA^{1*}, Guellala RIHAB¹, Rebai NOAMEN²

1. Laboratoire de Géoressources, CERTE, Technopole de BorjCedria Tunis, Tunisia.

E-mail : gannounisonia2017@gmail.com

2. University of Tunis El Manar, National School of Engineering of Tunis, Geotechnical Engineering and Georisk Research Laboratory (LR14ES03).B.P. 37, le Belvédère 1002, Tunis, Tunisia.

Abstract. The present study is an illustrative example highlighting the reliability of satellite imagery in the characterization of alluvial aquifers and, consequently, its valuable contribution to hydrogeological studies. It concerns the Tabarka region (northwestern Tunisia), marked by significant tourist activity with an excessive demand for water. Using Landsat ETM+ imagery, this study aims to enhance understanding of the Tabarka aquifer by mapping the tectonic lineaments influencing the Tabarka plain and the geometry of its aquifer system. The processing of satellite image, including enhancement, ACP, and their filtering based on different directions, reveals a total of 12 lineaments, mostly oriented NW-SE. Six lineaments are identified within the Tabarka plain (LP1, LP2, LP3, LP4, LP5, and LP6), whereas the others lie at its borders (LB1, LB2, LB3, LB4, LB5, and LB6). A digital terrain model (DTM) from the Aster GDEM V2 image was employed to discern the nature of these lineaments. We found that lineaments outlining the plain's edges are associated with topographic variations. Additionally, in the plain, most lineaments coincide with a notable decrease in aquifer resistivity, as evidenced in geoelectric sections incorporating lithological logs of water boreholes and interpreted vertical electrical soundings (VES). The identification of these lineaments may explain the presence of clay enrichment within the alluvial aquifer, thus reducing its suitability for exploitation between the Oughof and El Khebir rivers and in the eastern part of the plain. These lineaments may correspond to tectonic events controlling Quaternary sedimentation, thereby influencing the composition of alluvial deposits.

Keywords: Alluvial aquifer, Satellite imagery, Lineaments, Hydrogeology, aquifer geometry, Tabarka region, Tunisia.

Résumé. La présente étude est un exemple qui montre la fiabilité des images satellites dans la caractérisation des aquifères alluviaux et, par conséquent, sa contribution aux études hydrogéologiques. Elle concerne la région de Tabarka (nord-ouest de la Tunisie), marquée par une activité touristique significative ayant une demande excessive en eau. À l'aide de l'image Landsat ETM+, cette étude vise à mieux comprendre l'aquifère de Tabarka en cartographiant les linéaments tectoniques qui affectent la plaine de Tabarka et influencent la géométrie de son système aquifère. Le traitement de l'image satellite, l'amélioration, l'Analyse en Composantes Principales (ACP) et leur filtrage selon différentes directions révèlent au total 12 linéaments, majoritairement orientés NW-SE. Six linéaments sont détectés dans la plaine de Tabarka (LP1, LP2, LP3, LP4, LP5 et LP6), tandis que les autres se trouvent à ses frontières (LB1, LB2, LB3, LB4, LB5 et LB6). Un modèle numérique de terrain (MNT) provenant de l'image Aster GDEM V2 a été utilisé pour identifier la nature de ces linéaments. La superposition des linéaments identifiés avec ce modèle montre que ceux dessinant les bords de la plaine sont associés à des variations topographiques. Dans la plaine, la plupart des linéaments coïncident avec une notable diminution de la résistivité de l'aquifère observée dans les sections géoélectriques qui incorporent des forages d'eau et des sondes électriques verticaux interprétées (VES). La mise en évidence de ces linéaments pourrait expliquer l'enrichissement de l'aquifère alluvial en argiles et, par conséquent, la dégradation de son intérêt pour l'exploitation entre les rivières Oughof et El Khebir et dans la partie orientale de la plaine. Ils pourraient correspondre à des événements tectoniques contrôlant la sédimentation quaternaire et, par conséquent, la composition des alluvions.

Mots clés : Aquifère alluvial, imagerie satellitaire, linéaments, hydrogéologie, géométrie de l'aquifère, région de Tabarka, Tunisie.

INTRODUCTION

Alluvial aquifers worldwide represent valuable water resources due to their shallowness, vast extent, and essential reserves, contributing significantly to socio-economic development. Nevertheless, these aquifers are frequently affected by pollution and overexploitation. Preserving them requires a comprehensive understanding of both water quality and quantity. The reconstruction of aquifer geometry is of crucial significance for the development of hydrogeological models, allowing for the evaluation of reserves and playing a pivotal role in sustainable water resources management (MacDonald *et al.* 2012).

In Tunisia, where alluvial aquifers play a crucial role in drinking water supply and irrigation, this reconstruction is particularly important. Previous hydrogeological studies, such as the one conducted by Ben Dhia *et al.* (2014), underscore the importance of understanding the geometry of alluvial aquifers for assessing storage capacity and estimating available water resources. Furthermore, research carried out by Ben Hamouda *et al.* (2018), highlights the importance of alluvial aquifer geometry in modeling groundwater flows and predicting spatio-temporal groundwater variations. An accurate reconstruction of alluvial aquifer geometry in Tunisia is crucial for effectively managing risks associated with groundwater exploitation and optimizing the planning

of hydraulic infrastructures, as highlighted in the studies by Sghaier *et al.* (2016) and Ben Mammou *et al.* (2020). Additionally, the preservation of underground ecosystems in Tunisia also depends on a thorough knowledge of aquifer geometry, as highlighted by the work of Ben Hassen *et al.* (2019). An accurate reconstruction of the geometry of aquifers, particularly alluvial aquifers, is essential for sustainable water resource management, groundwater flow modeling, hydraulic infrastructure planning, and the preservation of unique underground ecosystems.

However, the tectonic events controlling the geometry of these aquifers may be absent on the geological map, requiring identification through various methods, such as geophysical studies, exploratory drilling, and electrical soundings. Geophysical studies, in particular seismic reflection, facilitate the characterization of alluvial formations properties and the reconstruction of the aquifer geometry (Ghassemi & Jakeman 2005). Exploratory drilling and the analysis of data from existing wells also provide valuable information on aquifer geometry (Chowdhury *et al.* 2017). In addition, the vertical electrical sounding (VES) technique is commonly used to measure the electrical resistivity of subsurface formations, offering information on the spatial distribution of aquifer layers (Moayedi 2016).

In recent years, remote sensing has considerably contributed to mapping lineaments and reconstructing the alluvial aquifer geometry. Indeed, satellite imagery, providing a synoptic view, emerges as a relevant solution for mapping lineaments associated with tectonic events (Lloyd 1999, Jourda *et al.* 2006, Hoffmann & Sander 2007, Meijerink *et al.* 2007, Youan 2008, Abdullah *et al.* 2014, Gannouni & Hamzaoui 2014, Adiri *et al.* 2017, Mathew & Ariffin 2018, Farahbakhsh *et al.* 2019, Christian *et al.* 2019, Epuh *et al.* 2020, Gobashy *et al.*

2023). A lineament is defined as a simple or compound linear line detected on the surface, whose individual parts, aligned along a straight line or curve, stand out clearly from their surroundings and possibly reflect a phenomenon generated beneath the surface (O'leary *et al.* 1976). It may correspond to structural elements such as faults, fractures, fold axes (Soesilo & Hoppin 1986), or to lithological contacts, topographic depressions, vegetation field boundaries, and hydrographic networks (Yatabe & Howarth 1984).

In this context, our study aims to reconstruct the geometry of the alluvial aquifer in the Tabarka plain, a region facing hydraulic constraints and specific challenges in water supply. Understanding aquifer geometry is crucial for assessing both the quantity and quality of available groundwater and for optimizing its management. To achieve this objective, our research focuses on identifying various lineaments in the study area, which play a significant role in the arrangement of permeable deposits, geological formations capable of storing and transmitting water. To identify and characterize these lineaments, we utilized spatial data from Landsat ETM (Enhanced Thematic Mapper) and Aster GDEMv2 (Global Digital Elevation Model Version 2) satellites. The use of remote sensing methodologies offers a unique advantage, providing a comprehensive and synoptic view of the region, including inaccessible areas. This approach allows for the examination of large-scale patterns and features that may not be readily observable through traditional ground-based surveys alone. This innovative methodology enables us to gain insights into the aquifer's structure and dynamics, contributing to the planning and sustainable management of water resources in the region by facilitating informed decisions regarding the use and protection of groundwater.

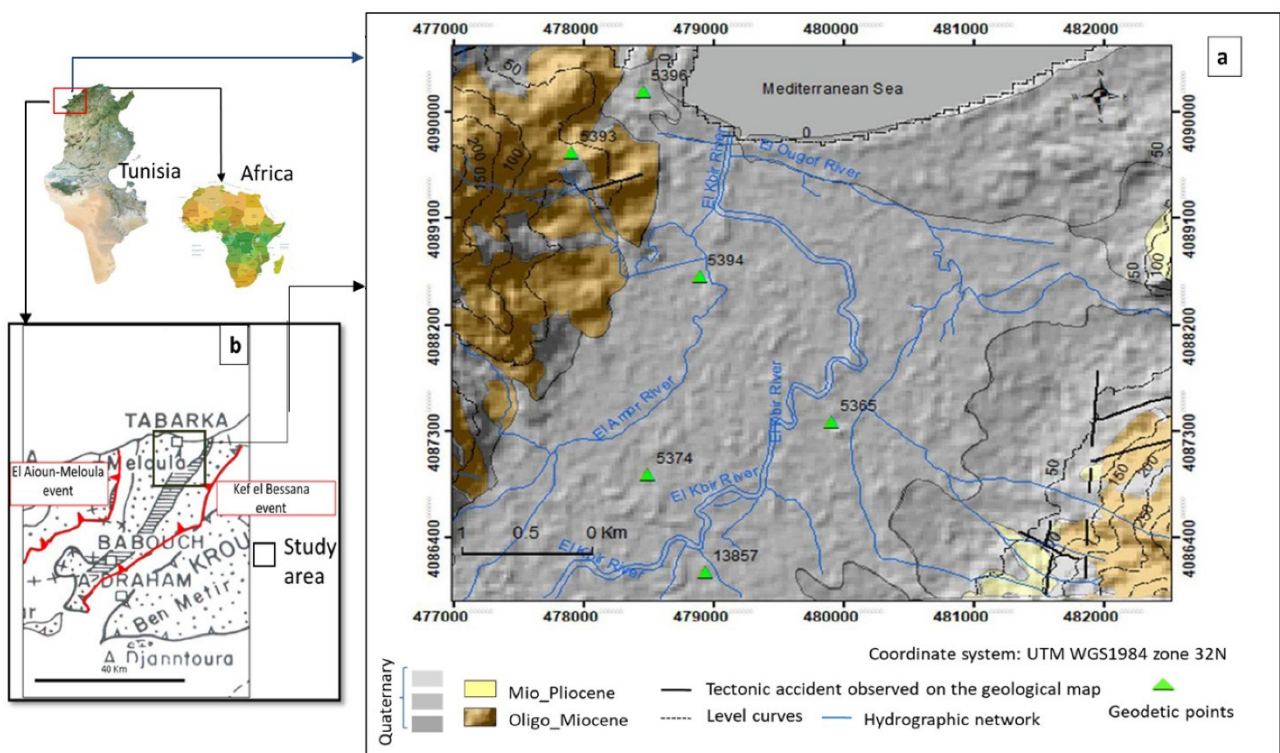


Figure 1. a) Tabarka geological map (Rouvier and Ben Salem 1992), b) Structural setting of the Tabarka plain (Rouvier 1977).

REGIONAL SETTING

Geology

The Tabarka plain is a coastal area (Fig. 1a) located 175 km from Tunis. Geologically, it is defined as a synclinal structure (Rouvier 1977), with Quaternary filling made of dune sands, clays, pebbles, silts and gravels. It is bordered by Oligo-Miocene deposits composed of Kroumirie sandstones and Babouch clays. These deposits corresponding to the Numidian flysch (Rouvier 1977, Rouvier & Ben Salem 1992, Riahi *et al.* 2010, Talbi *et al.* 2008), essentially outcrop in the Tellian domain, also called the “zone of thrust nappes” (Rouvier 1977). The contact of the Numidian formation with its substratum is controversial. It is considered a sedimentary contact by Kujawski (1964), Crampon & Sigal (1967), Crampon (1971, 1973) and Salaj *et al.* (1974), while it is a tangential abnormal contact according to Jauzein (1962), Rouvier (1977), El Euchi *et al.* (2004), Ould Bagga *et al.* (2006), Boukhalfa *et al.* (2009) and Riahi *et al.* (2010).

The Tabarka plain belongs to the Babouch –Tabarka syncline extending over 25 Km and narrows from north to south (Rouvier 1977). The western flank of this syncline is affected by the El Aioun- Meloula fault, oriented N-S in the northern part and NE-SW in the southern part. Its eastern flank, truncated by Kef El Bessana fault, is overturned towards the northwest (Fig. 1b)

Hydrogeology

From a hydrogeological point of view, the Tabarka plain exhibits two discernible aquifer systems, as highlighted in the study conducted by Guellala *et al.* (2017) focusing on the Tabarka region. The first aquifer is a phreatic water table composed of dune sands that cover the northern part of the plain. This water table is characterized by its excellent water quality. In addition, the above-mentioned study highlights the existence of a deep alluvial aquifer, sustained by the El Kebir river and its tributaries, notably the Oughof and Amor rivers.

It is important to note that this deep alluvial aquifer in the Tabarka plain displays geographical variations in its composition. According to Guellala *et al.* (2017), this aquifer experiences an enrichment in clays from the southern to the northern regions, leading to a notable decrease in both flow rates and permeability coefficients in that direction.

Datasets and Methodology

The adapted methodology consists of several steps (Fig. 2):

Data acquisition

Semi-automatic extraction of lineaments: Use linear feature extraction techniques to identify lineaments from Landsat images.

Utilization of ASTER GDEM and DTM (Digital Terrain Model): Integrate ASTER GDEM and DTM data to validate the extracted lineaments. Compare detected lineament locations with identified topographic variations to evaluate their coherence.

Topographic maps: Use topographic maps to eliminate anthropogenic lineaments. Identify and exclude linear infrastructures (e.g., roads, pipelines) from the analysis to focus on natural lineaments.

Lineament mapping: Create a map of lineaments by integrating all extracted, validated, and corrected information from the previous steps. This map visually represents identified lineaments in the study area.

Validation of results: Compare surface lineaments with resistivity variations identified from geoelectrical cross sections.

Datasets

Various data types are used in our study, namely spatial, surface and subsurface data. Spatial data include a Landsat 7 ETM+ satellite image (Fig.3) and Aster GDEM V2 (Table 1). The Landsat 7 ETM+ image consists of a 15 m spatial

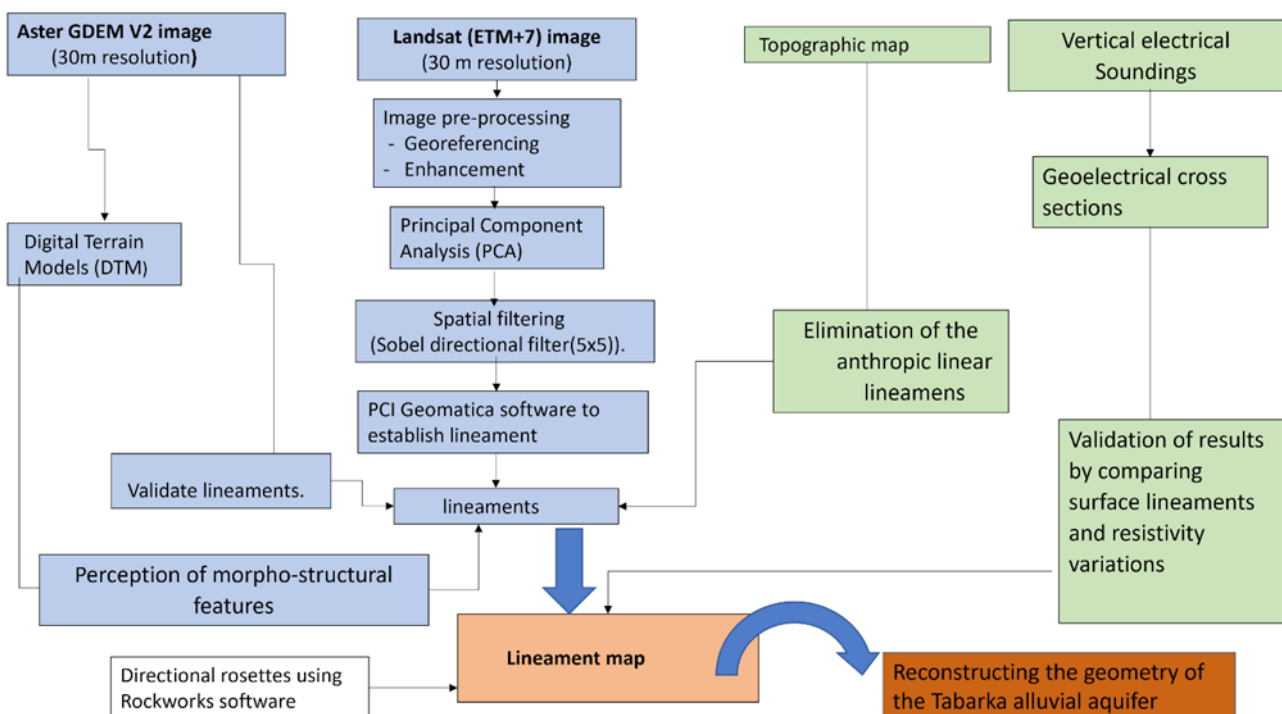


Figure 2. Research Methodology Framework.

resolution TM 8 panchromatic band and six multispectral bands (TM 1, 2, 3, 4, 5, 7, with 30 m spatial resolution), and a 120 m spatial resolution TM 6 band. Only the six multispectral bands (TM 1, 2, 3, 4, 5, 7, with 30 m spatial resolution) were resampled to make them superposable on the Aster GDEM V2 image with a 30 m resolution. The Landsat image is selected for its spectral and spatial characteristics, allowing good small-scale structural mapping (Youan *et al.* 2008). The use of the Landsat image is attributed to its low solar angle value, its ability to suppress disturbing spatial detail, and its regional coverage (Sabins 1986). The image is taken on the 6th of June 2016, a period corresponding to the dry season characterized by an almost total absence of clouds, contributing to better visibility of the sensors. Surface data describing the distribution of hydrographic features and geological outcrops are extracted from Tabarka topographic and geological maps. The subsurface data consists of 25 vertical electrical soundings (VES) and five water boreholes (Fig. 4). They were provided

by the Regional Commissariat of Agricultural Development (CRDA) of Jendouba and the General Directorate of Water Resources (DGRE). The VES measurements were selected at 25 sites according to the location of the identified lineaments. The Schlumberger array was used for VES acquisition, considering a maximum electrode spacing of 1000 m. Five water boreholes exploiting the Quaternary aquifer system in the Tabarka plain were consulted. We have mainly used the lithological columns described in the final reports of these borehole's execution (Ouertani 1978, Balti & Ghazouani 1989, Hezzi & Ghazouani 1996, Kallali *et al.* 2006, Balti & Manai 2009).

A greater number of vertical electrical soundings (30 VES) and water boreholes (eight water boreholes, including lithological columns and well logs), were previously used to identify the Quaternary water reservoirs within the Tabarka plain and reconstruct their geometry (Guellala *et al.* 2017).

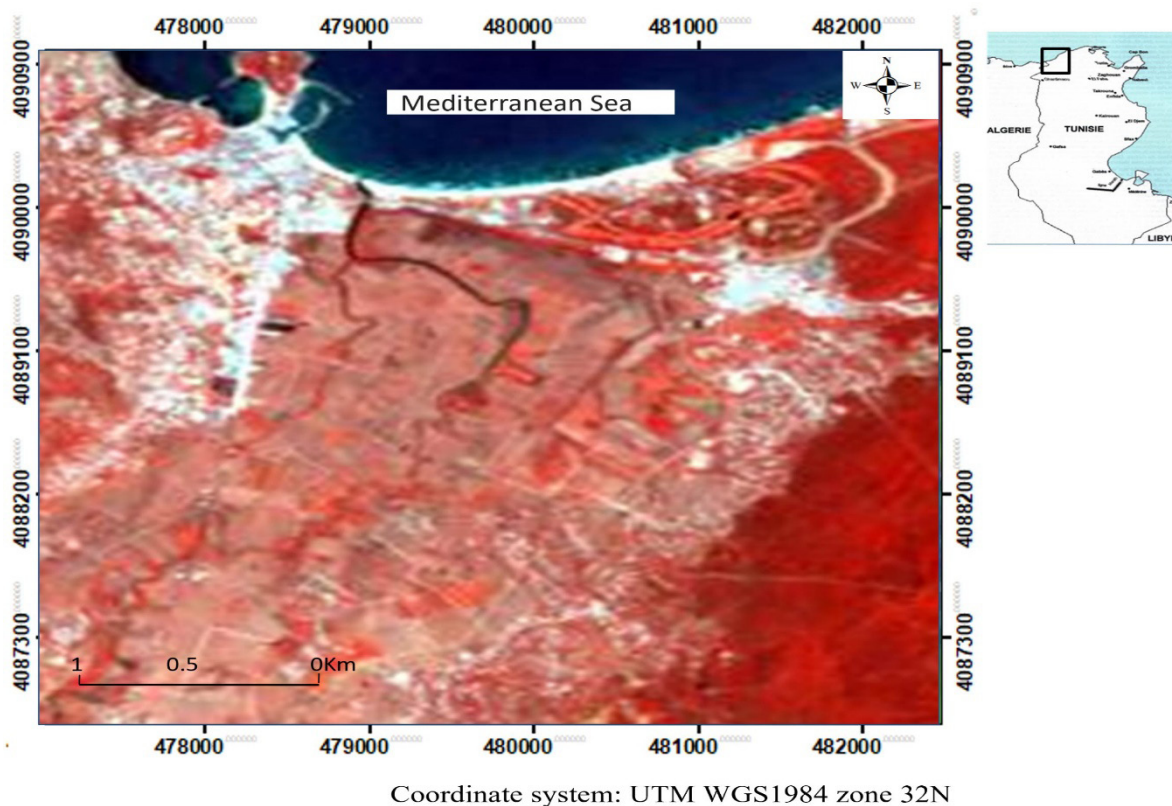


Figure 3. The color composition of bands 4.2.1 of the Landsat7 ETM++ image of 10/06/2016.

Table 1. Summary of the datasets

Image Types	Date	Spatial Resolutions	Sources
Landsat 7 ETM (Enhance Thematic Mapper)	Acquisition date: 10 /6/ 2016	Band (1, 2, 3, 4,5et 7) : 30 m Bande6 : 60 m Pan : 15m	https://earthexplorer.usgs.gov/
ASTER GDEM V2 (Global Digital Elevation Map)	Publication date: 1/10/2012	The GDEM had 1 arc-second latitude and longitude postings (~30 m), and a vertical accuracy of approximately 10 m. The data were tiled as 22.000+ 1 × 1 degree latitude/longitude files each accompanied by a quality file.	Http:// emex.cr.gov/DEMEX/

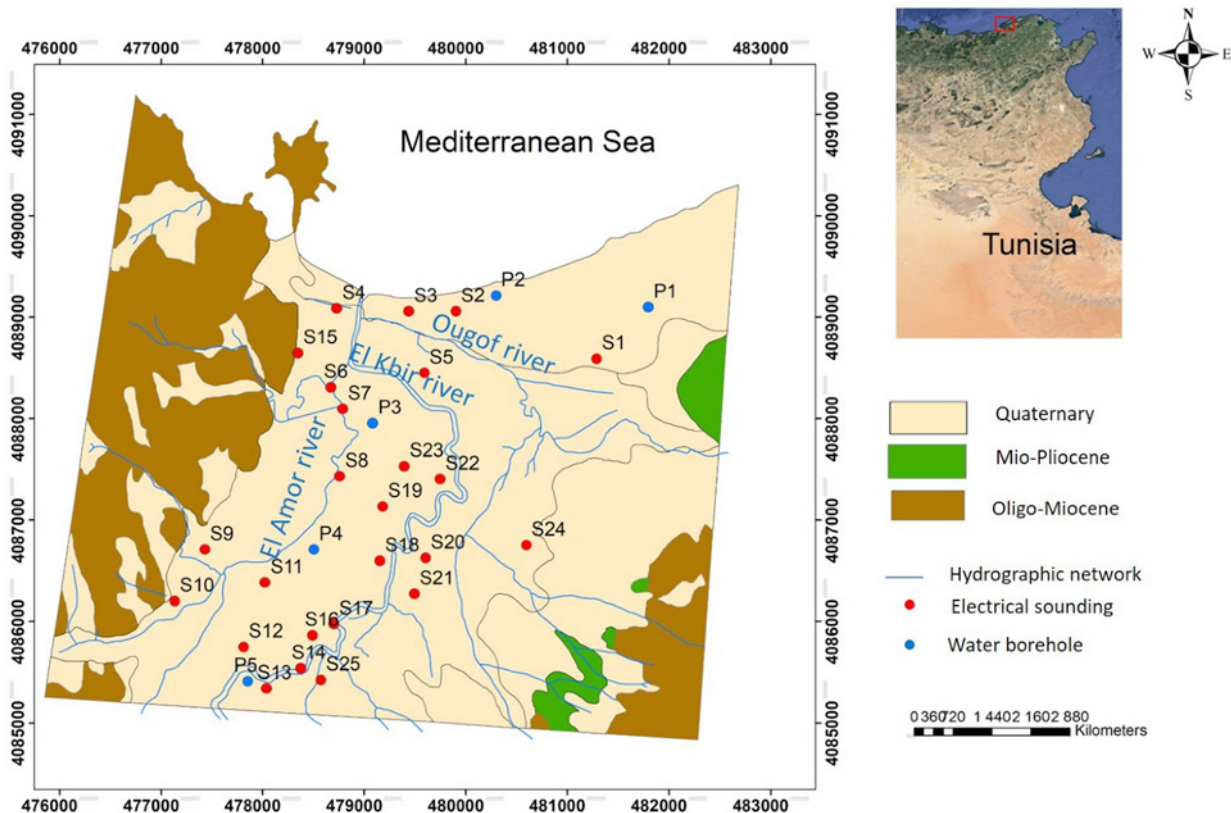


Figure 4. Distribution of the used water boreholes and vertical electrical soundings

Methodology

Different processing techniques were successively applied to the satellite image using different software tools for lineaments extraction (Fig. 2). We are initially georeferenced the raw image and then applied image enhancement techniques for visual improvement. Principal Component Analysis (PCA) was employed to reduce redundancy, manage data size, and explore correlations between images (Bonn & Rochon 1992). The application of the PCA showed that the first three new principal components (PC1, PC2, and PC3) provided respectively 90.28%, 6.73%, and 2.80% of the satellite image information, totaling 99.81% (Fig. 5). Subsequently, spatial filtering of the data was carried out using the Sobel directional

filter. This involves applying a convolution to the image, resulting in modifications to the pixel values at coordinates (x, y) (O'leary *et al.* 1976, Prost 2001, Laake 2011). Directional filters are widely used in geology to detect lineaments (Kouamé *et al.* 1999 and 2005, Javhar 2019).

Sobel directional filters at 0°, 45°, 90°, 135° were applied to the main components from the PCA and the six multispectral bands (TM 1, 2, 3, 4, 5, 7). This process enhanced contours and highlighted the directions of geological discontinuities in the image. A 5 x 5 matrix was chosen in this study, generating images with sufficient detail for lineament detection (Table. 2).

Table 2. Matrix of 5*5 Sobel directionnel filters.

Sobel directional filter NW-SE				
3	2	2	1	0
2	4	3	0	1
2	3	0	3	2
1	0	3	4	2
0	1	2	2	3

Sobel directional filter NE-SW				
0	1	2	2	3
1	0	3	4	2
2	3	0	3	2
2	4	3	0	1
3	2	2	1	0

Sobel directional filter E-W				
1	1	0	1	1
2	3	0	3	2
2	3	0	3	2
2	3	0	3	2
1	1	0	1	1

Sobel directional filter N-S				
1	2	3	2	1
1	3	4	3	2
0	0	0	0	0
1	3	4	3	2
1	2	3	2	1

The images resulting from processing with directional filters are then imported into the PCI Geomatica software (PCI, Geomatica 2001) to establish lineament maps of the study area. The maps that highlight the most discontinuities are the CP1 map and the filtered band four map. They allow the identification of extracted lineaments such as veins, panels, dykes, and faults. Overlaying with the topographic map involves geoprocessing to eliminate all linear structures of anthropic origin detected on the image, including roads, tracks, and high-voltage lines. Finally, the overlay of the lineaments identified on the filtered band 4 allows the creation of the lineament map (Fig. 6). Directional rosettes, proportional to the cumulative length of the lineaments and organized into 10° classes, are generated from the neo-data resulting from GIS calculations using Rockworks software (De Dreuzy 2000) (Fig. 6).

There is complementarity in spatial data, as the ETM+7 image is used for its spectral particularities to highlight the overall state of fracturing. The use of the SRTM image was a part of verifying the strength of the filters used, given the SRTM image has the advantage of not being altered by the atmosphere or other meteoric factors (Coulibaly 2021). We have used it to validate certain lineaments. On the other hand, it is also used for the development of DTM numerical models that aim to facilitate the perception of morpho-structural ensembles in the studied domain and map them. Thus, geomorphological variations are major witnesses of the morphogenetic evolution of reliefs, which can be used to identify geological forms such as collapse ditches, plateaus, and extract morpho-structural discontinuities (Bonnet & Colbeaux 1999, Deffontaines 2000).

Moreover, to identify lineaments corresponding to subsurface discontinuities, we constructed interpretations

from lithological columns of water boreholes and interpreted vertical electrical soundings (VES), geoelectrical cross-sections, and the aquifer extension map (Guellala *et al.* 2017).

It should be noted that VES is a survey technique of the electrical resistivity method of geophysical prospecting, involving the injection of an electric current into the ground and measuring the resulting potential difference between pairs electrodes (Dobrin 1976, Telford *et al.* 1976, Nazih *et al.* 2022).

The apparent resistivity values, deduced consequently, were interpreted using the theoretical master curves and inversion software such as IPI2 WIN and WINSEV to obtain true resistivity and thickness (Fig. 7).

RESULTS

Following directional filtering, 12 lineaments, mostly oriented NW-SE, are extracted (Fig. 8). The lineaments LP1, LP2, LP3, LP3, LP4, LP5, and LP6 are detected in the plain, while (LB1, LB2, LB3, LB4, LB5, and LB6) are observed at its edges. The superposition of the identified lineaments on the digital terrain model (Fig. 9) shows that those at the edges of the plain are associated with topographic elevations. Lineaments LB1 and LB3 delineate the boundary between the Tabarka plain and the Mediterranean Sea; in northern Tunisia, marine deposits that outcrop in coastal regions are often intensely deformed (Mejri 2012), while LB2 and LB4 delimit the island located in the northwest of this plain. The submeridian lineament LB5, located on the Oligo-Miocene outcrop bordering the plain to the west, intersects three contours; its northern extremity lies between the 200 and 150 m curves, while the rest mainly falls between 150 and 100 m. The LB6 lineament, located at the eastern edge of the plain,

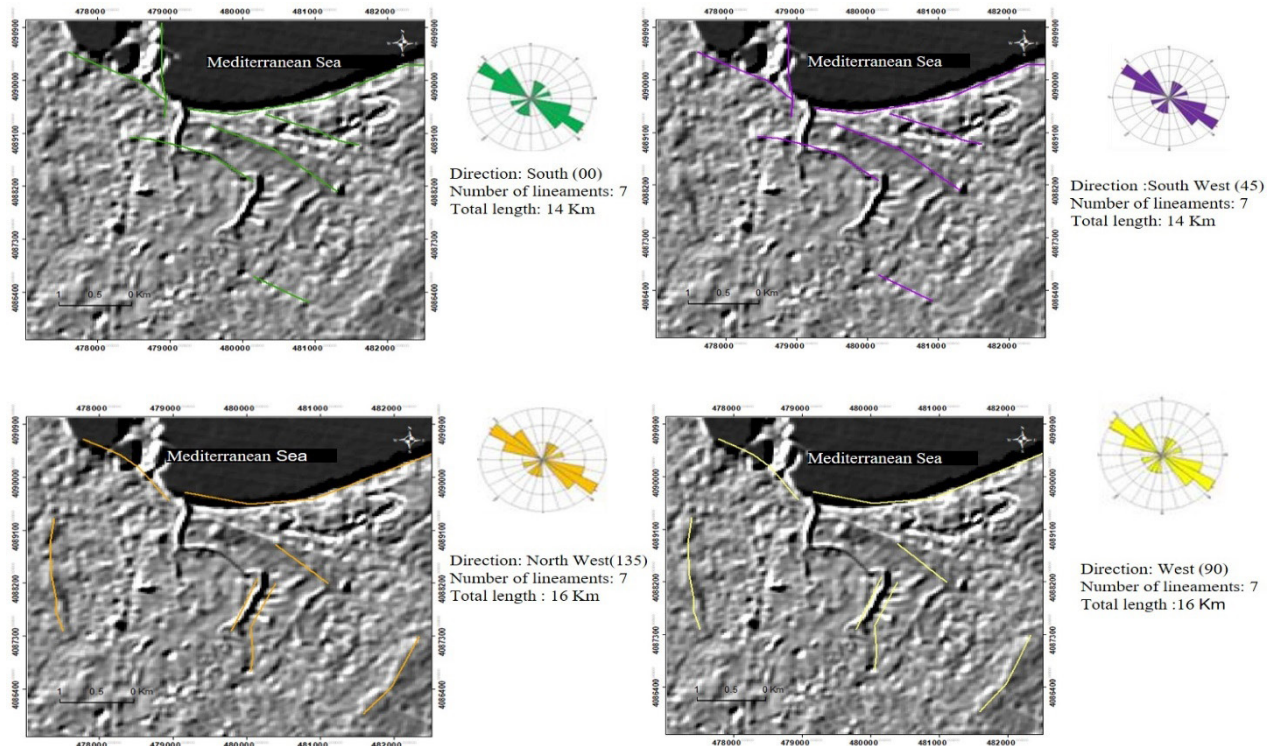


Figure 6, Maps and directional rosettes of the lineaments obtained from the filtering according four directions: N-S, NE-SO, E-O ET NO-SE. (coordinates are in UTM Zone 32N).

marks the transition between the 150m and 100m elevations. The altitudes do not show significant variation; being less than 50 m. This may suggest that the lineaments detected in this plain do not correspond to topographical variations but rather to tectonic events (Rouvier & Ben Salem 1992). LP1, the northernmost lineament in the plain, is identified in the dunes, indicating the presence of geological rocks different from the sands that mainly constitute these dunes. Aeolianites with decarbonization chimneys and red clayey sands have already been observed in the field (Paskoff & Sanlaville 1983). LP2 marks the southern limit of the dunes, corresponding to a lithological change between the dunes and the alluvia, mainly composed of gravel and clay. It coincides with the downstream part of the Oughof river. Equally, LP3 covers the northern part of the El Kebir river, while LP4 corresponds to the NNE-SSE junction of the El Kebir river. The submeridian LP5 separates this river and the Oughof river. The LP6 lineament is identified in the southeastern part of the plain, between two tributaries of the Oughof river, indicating an old watercourse (Rouvier & Ben Salem 1992). In light of the results obtained from the analysis of the lineaments, which have highlighted their influence on the geometry of the Tabarka alluvial aquifer, it is crucial to validate these findings. Therefore, we have undertaken a second phase of the study, focusing on the comparison with the results obtained from electrical resistivity surveys. This approach will allow us to further consolidate and thoroughly confirm the initial observations, thus deepening our understanding of the aquifer's structure. In light of these findings and their implications for the Tabarka alluvial aquifer's geometry, validation is essential. Therefore, a second phase of the study will focus on comparing these results with data obtained from electrical resistivity surveys. This approach aims to strengthen and confirm the initial observations, thereby enhancing our understanding of the aquifer's structure and dynamics.

Validation and Discussions

To assess the influence of the identified lineaments on the geometry of the Tabarka alluvial aquifer, we established geoelectrical cross-sections traversing different lineaments in the plain. The most representative ones has been selected for analysis. The transverse geoelectrical cross-section for the LP2 and LP3 lineaments integrates the electrical soundings S2 and S5, and the water boreholes P2 and P3 (Fig. 10). It illustrates that the dune aquifer and the alluvial one are recognized in the P2 borehole, representing resistivities of 950 Ohm.m and 29 Ohm.m beneath VES 2. Passing to VES 5, these values drop to 1.5 and 10 Ohm.m suggesting a notable enrichment in clays. At the P3 borehole, occupying the southwestern extremity of the section, the alluvial aquifer is intersected at 32 m. The remarkable decrease in resistivity between the El Kebir river and the Oughof river, indicating a change in aquifer composition, coincides with the lineaments LP2 and LP3 identified within the Tabarka plain. Another geoelectrical cross-section, perpendicular to LP5 and passing through the electrical soundings S24 and S20 (Fig. 11), reveals that this lineament corresponds to a significant variation in the resistivity of the alluvial aquifer. In fact, VES 20 recognizes this aquifer with a resistivity of 40 Ohm.m, while VES 24 exposes only conductive layers of 2 and 5 Ohm.m.

The extension map of the Tabarka alluvial aquifer, derived from lithological logs of water boreholes and interpreted vertical soundings (Guellala et al. 2017), unveils areas unsuitable for exploitation in two primary zones (Fig. 12). The first zone (A) spans between the Oughof and El Kebir rivers, while the second (B) lies in the eastern part of the plain. Overlaying the lineament map resulting from satellite image processing (Fig. 8) onto this map reveals how the identified lineaments delineate boundaries between areas of interest and those less favorable for aquifer exploitation. Specifically, LP2 and LP3 outline zone (A), while LP5 marks the boundaries

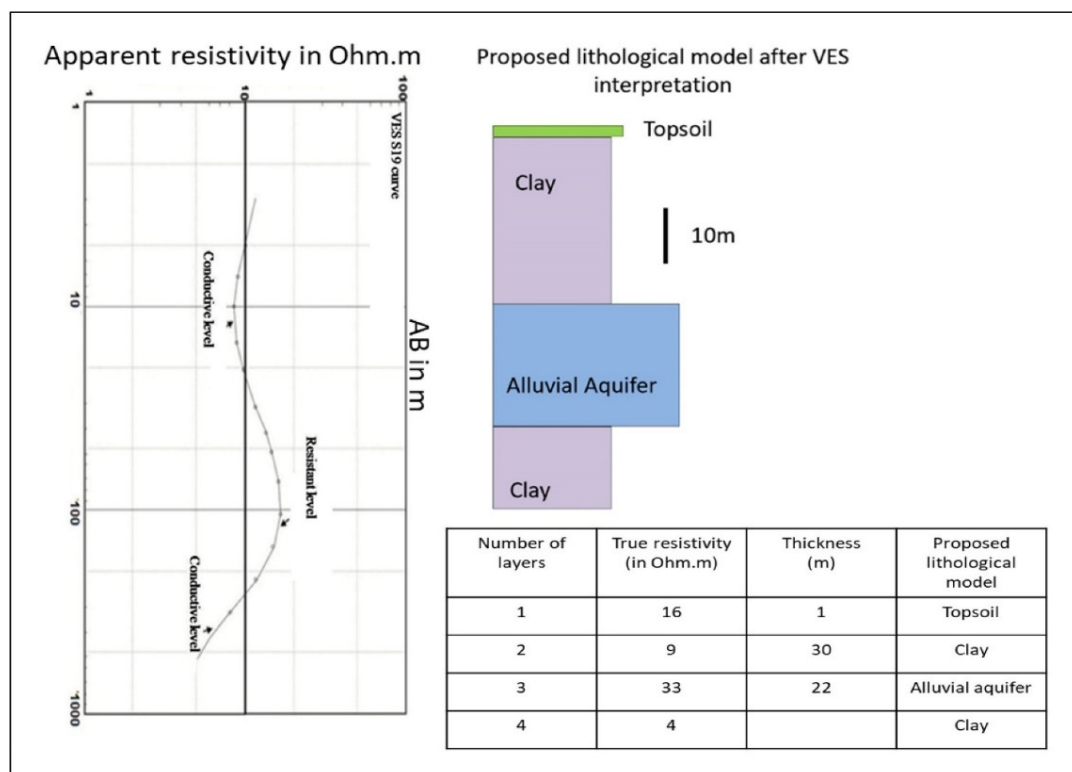


Figure 7. Interpretation of a vertical electrical sounding: example of VES S19(VES interpretation was performed as part of this study).

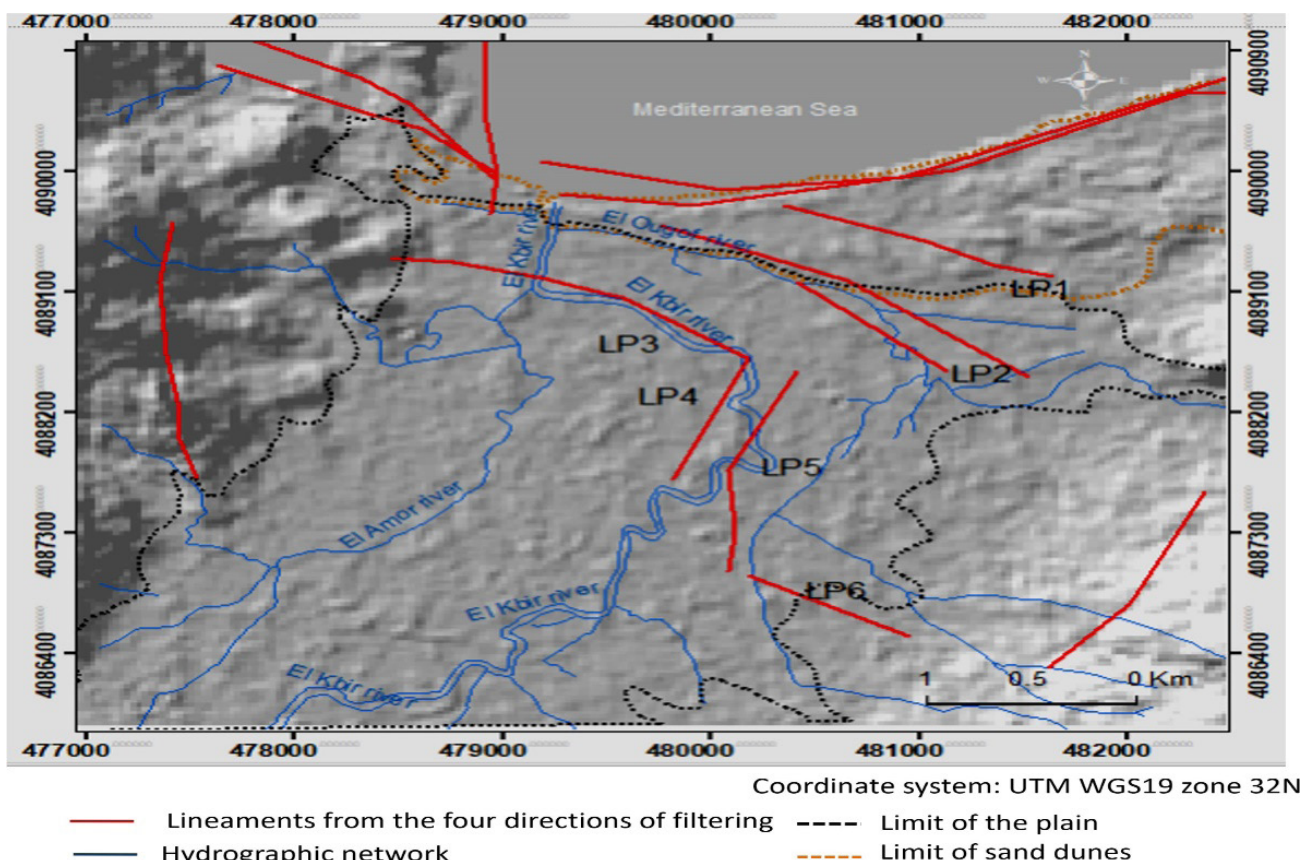


Figure 8. Synthesis map of the identified lineaments

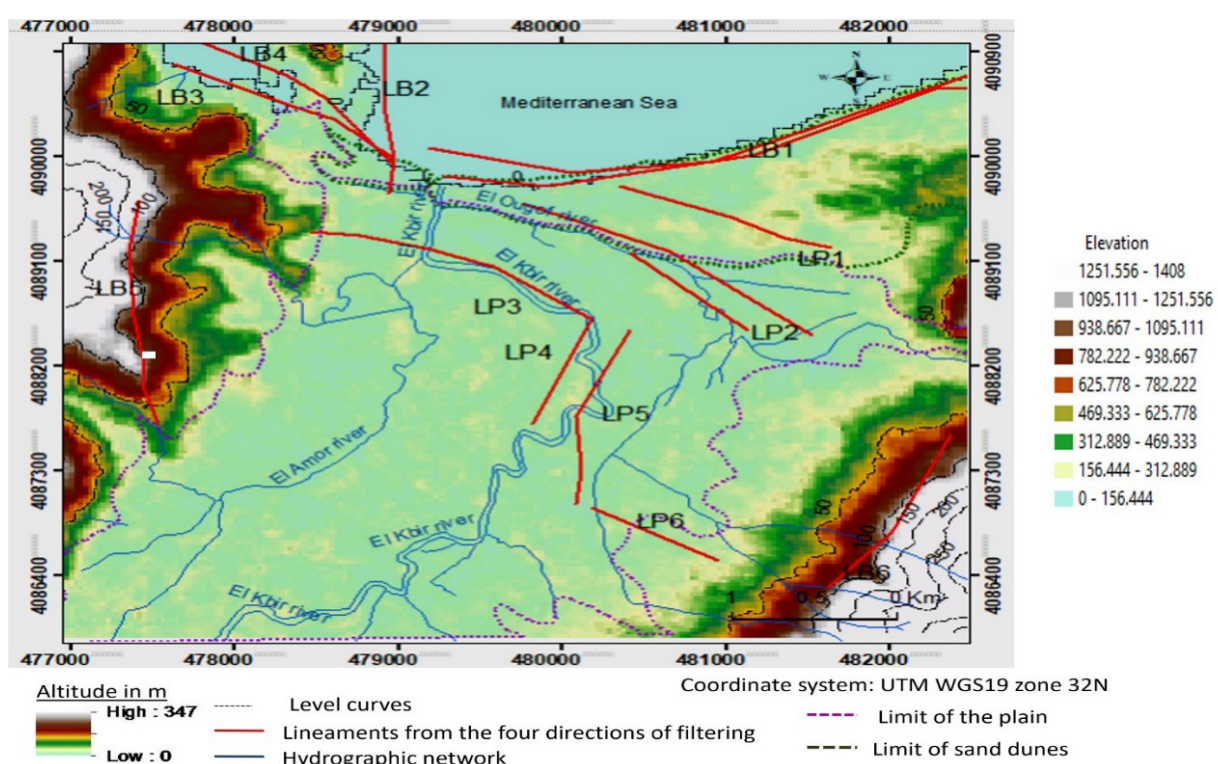


Figure 9. Superposition of the identified lineaments on the digital model of terrain (DTM created from ASTER GDEM V2 image of 1/10/2012).

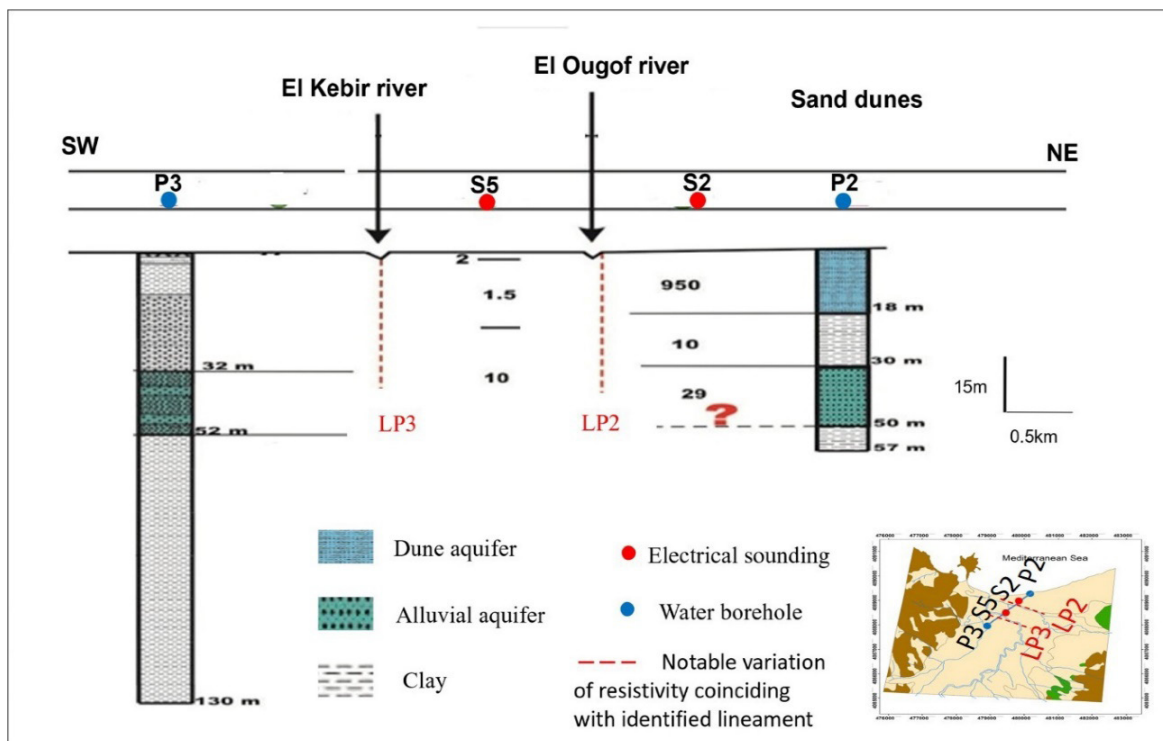


Figure 10. Geoelectrical cross section transverse to the lineaments LP2 and LP3 (The resistivities are in Ohm. m).

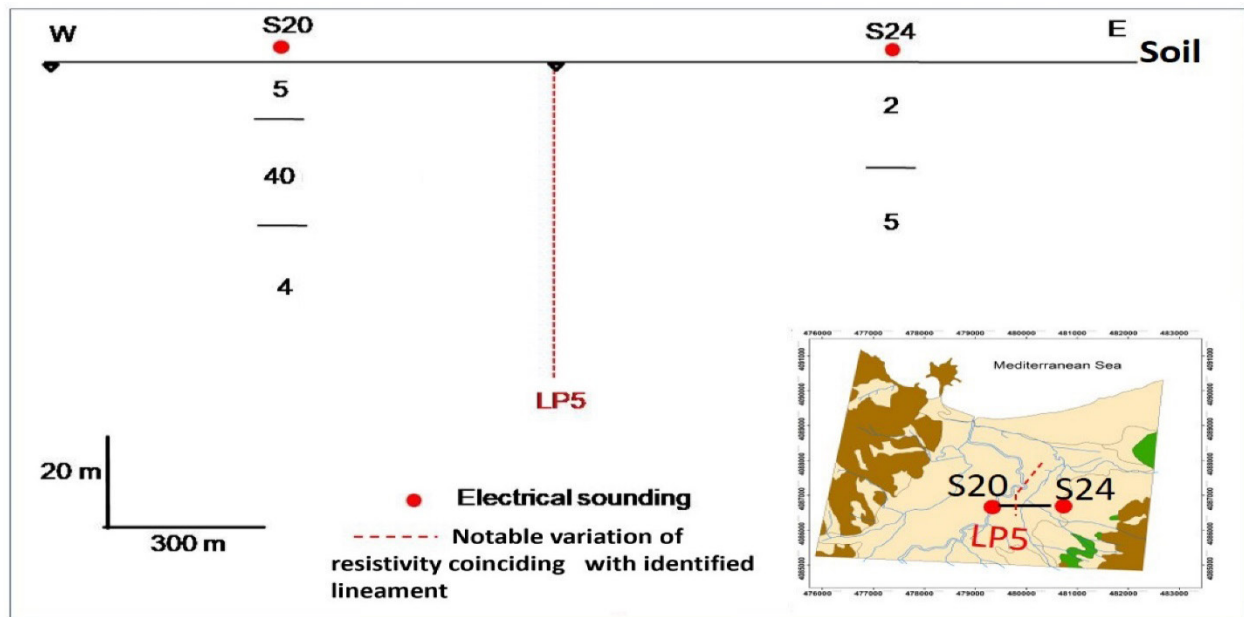


Figure 11. Geoelectrical cross section transverse to the lineament LP5 (The resistivities are in Ohm. m).

of zone (B). The detection of these lineaments elucidates a significant decrease in alluvial aquifer resistivity within both zones (A) and (B), indicative of clay enrichment. These lineaments are interpreted as normal synsedimentary faults that have created downthrown compartments between the Oughof and El Kebir rivers and east of the plain, facilitating the accumulation of thick clay layers. The synsedimentary activity, driven by NW-SE and N-S tectonic events during the recent Quaternary extension phase, has been observed in various plains across northern Tunisia (Rouvier 1977, Ben Ayed 1986), significantly influencing the geometry of the

Quaternary aquifer (Guellala *et al.* 2012). Moreover, these highlighted lineaments have influenced the course of rivers supplying the Tabarka alluvial aquifer, as evidenced by the directional shifts of the Oughof and El Kebir rivers aligning with LP2, LP3, and LP4 lineaments. Numerous authors have underscored the tectonic control exerted over the hydrographic network in Tunisia (Ben Ayed 1986, Kadri & Ben Haj Ali 1999 Amiri 2012) and globally (Genna *et al.* 1997, Roux & Harmand 1998, Larue 2005).

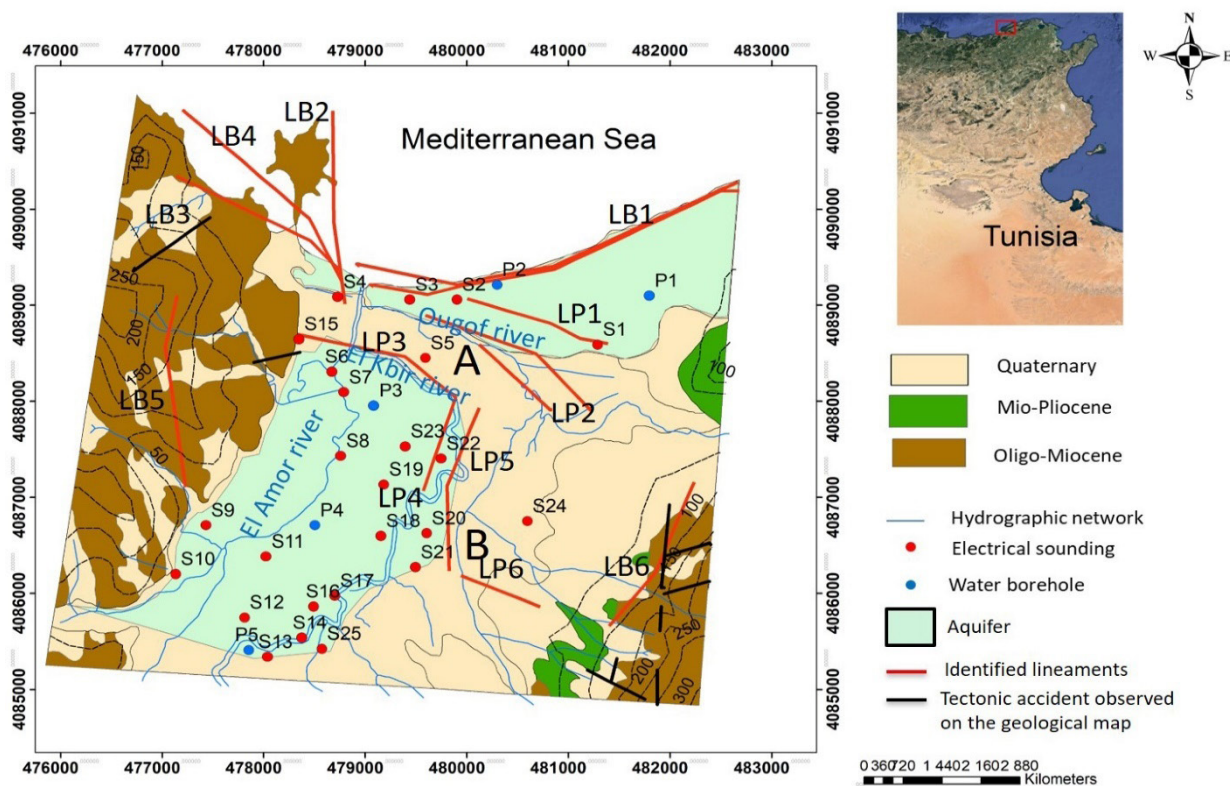


Figure 12. Superposition of the highlighted lineaments on the aquifer extension map.(Geological map).

CONCLUSION

The integrated use of satellite imagery, water boreholes, and vertical electrical soundings has significantly enhanced the hydrogeological schema of the Tabarka region. The analysis of satellite images revealed linear features in the Tabarka plain, which were subsequently overlaid onto the digital terrain model. Notably, these linear features, located along the edges of the plain, correlated with topographic elevations, while those within the plain coincided with notable variations in the resistivity of the alluvial aquifer, as revealed by geoelectric sections.

The identification and emphasis on these linear features are crucial, clarifying the change in the alluvial aquifer composition between the Oughof and El Khebir rivers, as well as in the eastern part of the plain. In these areas, the aquifer is considered uninteresting for exploitation, and these linear features may likely correspond to tectonic faults controlling the sedimentation of the permeable Quaternary deposits.

In conclusion, the use of satellite imagery in this study demonstrates its significance and reliability in reconstructing the geometry of alluvial aquifers. The delineation of linear features from satellite images has proven instrumental in identifying the Tabarka aquifer's areas of interest for exploitation.

This approach offers numerous advantages, including broad spatial coverage, accessibility to inaccessible areas, multispectral data, temporal monitoring, cost-effectiveness, ease of use, and the validation of existing models, contributing to effective water resource management planning. These results position this study as a noteworthy international reference for the application of satellite imagery in characterizing alluvial aquifers, particularly in scenarios with limited available data.

ACKNOWLEDGMENT

The authors would like to express their gratitude to the editor of «Bulletin de l'Institut Scientifique» ACHAB mohammed and the anonymous reviewers for their significant contribution to the improvement of the manuscript.

REFERENCES

- Abdullah A., Nasser S. & Ghaleeb A. 2013. Landsat ETM-7 for Lineament Mapping using Automatic extraction technique in the SW part Taiz area, Yemen. *Global Journal of Human Social Science Geography, Geo-Sciences, Environmental & Disaster Management*, 13, 3, 35-38.
- Adiri Z., El Harti A., Jellouli, A. et al. 2017. Comparison of Landsat-8, ASTER and Sentinel 1 satellite remote sensing data in automatic lineaments extraction: A case study of Sidi Flah- Bouskour inlier, Moroccan Anti Atlas. *Advances in Space Research*, 60, 11, 2355-2367.
- Amiri A. 2012. *Apport des méthodes géophysiques à la modélisation géodynamique de la moyenne vallée de la Mejerda*. Thèse de Doctorat, Université de Tunis II.
- Balti N. & Ghazouani L. 1989. *Compte Rendu de fin de travaux du forage Montazeh Tabarka*. Rapport interne, Direction Générale des Ressources en Eau.
- Balti N. & Manai K. 2009. *Compte Rendu de fin de travaux du forage Hotel Mehari Tabarka*. Rapport interne, Direction Générale des Ressources en Eau.
- Ben Ayed N. 1986. *Evolution tectonique de l'avant-pays de la chaîne alpine de Tunisie du début du Mésozoïque à l'actuel*. Thèse de Doctorat en sciences Naturelles, Université Paris Sud Orsay.
- Ben Dhaia H., Abida H. & Leduc C. 2014. Estimation de la géométrie des nappes alluviales de Kairouan (Tunisie centrale) à partir

- de la prospection géophysique et des données de piézométrie. *European Scientific Journal, ESJ*, 10,4.
- Ben Hamouda M. F., Trabelsi R., Jallouli C. et al. 2018. Numerical modeling of groundwater flow and contaminant transport in the shallow aquifer of Kairouan, central Tunisia. *Environmental Earth Sciences*, 77,6, 236.
- Ben Hassen W., Souid H., Slimani R. et al . 2019. Groundwater-dependent ecosystem dynamics in the semi-arid region of the Medjerda River Basin, Tunisia. *Ecohydrology*, 12,2, e2062.
- Ben Mammou A., TrabelsiR., JallouliC. et al. 2020. Groundwater vulnerability assessment using DRASTIC and GIS techniques in the semi-arid region of Kairouan, central Tunisia. *Arabian Journal of Geosciences*, 13,5, 1-14.
- Bonn F. & Rochon G. 1992. Précis de télédétection volume 1: Principes et méthodes. Sainte- Foy: Presse de l'université du Québec/AUPELF, 485 p.
- Boukhalfa K., Ismail-Latrache K.B., Riahi S. et al. 2009. Analyse biostratigraphique et sédimentologique des séries éo-oligocènes et miocènes de la Tunisie septentrionale: implications stratigraphiques et géodynamiques. *Comptes Rendus. Géoscience*, 341,1, 49– 62.
- Bonnet T. & Colbeaux J. P. 1999. L'analyse morphologique spatialisée: apport d'une méthode à la détection des accidents, une nécessité dans l'approche hydrodynamique karstologique des aquifères fissurés. Exemples dans le nord de la France crayeux. *Geodynamica Acta*, 12, 3-4, p. 223-235.
- Chowdhury A., Jex C. N. & Shamsuddoha M. 2017. Alluvial aquifer systems in Asia: A review. *Hydrogeology Journal*, 25,5, 1359-1381.
- Christian A., Sekouba O., Alexis K. et al. 2019. Extraction automatique des linéaments à l'aide d'images satellitaires optique et radar en milieu de socle précambrien (Haute Marahoué, Côte d'Ivoire). *International Journal of Engineering Science Invention*, 8, 1, 24-32. Online ISSN : 2319 – 6734.
- Crampon N. & Sigal J. 1967. Stratigraphie du Crétacé terminal et de l'Eocène en bordure des Mogods (Tunisie septentrionale). *Bulletin de la Société Géologique de France*, 11,129-140.
- Crampon N. 1971. *Etude géologique de la bordure des Mogods du pays de Bizerte et du Nord des Hédir (Tunisie septentrionale)*. Thèse de Doctorat, Université Nancy 1, 522 p.
- Crampon N. 1973. L'Extrême Nord-tunisien, Aperçu stratigraphique pétrologique et structural, in Livre Jubilaire Marcel Solignac. *Annales Mines et Géologie Tunis*, , 26,49-85.
- Coulibaly H.S.P., Honore C. T. J., Naga C. et al. 2021. Groundwater exploration using extraction of lineaments from SRTM DTM and water flows in Béré region. *Egyptian Journal of Remote Sensing and Space Sciences*, 24 ,3, 391-400. Online ISSN: 1110-9823.
- De Dreuzy J.R . 2000. *Analyse des propriétés hydrauliques des réseaux de fractures*, Université de Rennes. Thèse de doctorat, Université Rennes 1, 101 p.
- Deffontaines B. 2000. *Formes et déformations de la surface terrestre : approche morphométrique et application*. Thèse d'habilitation à diriger la recherche. Université Pierre et Marie Curie, 65p.
- Dobrin M.B. 1976. *Introduction to geophysical prospecting*. 3rd Edition, McGraw Hill, New York.
- Epuh E.E., Okolie C.J., Daramola O.E et al. 2020. An integrated lineament extraction from satellite imagery and gravity anomaly maps for groundwater exploration in the Gongola basin. *Remote Sensing Applications journal: Society and Environment*, 20,100346. <https://doi.org/10.1016/j.rsase.2020.100346>.
- El Euchi H., Saidi M., Fourati L. et al. 2004. Northern Tunisia Thrust Belt: Deformation Models and Hydrocarbon Systems. In: Deformation, fluid flow, and reservoir appraisal in foreland fold and thrust belts (Swennen, R.; Roure, F. & Grnath, J.W. eds.). *American Association of Petroleum Geologists (AAPG), Hedberg Series*, 1, 371-390.
- Farahbakhsh E., Chandra R., Olieroor K.H. et al. 2019. Computer vision-based framework for extracting tectonic lineaments. *International Journal of Remote Sensing*, 41,5,1760-1787. <https://doi.org/10.1080/01431161.2019.1674462>.
- Gannouni S. & Hamzaoui F. 2014. Identification de couloirs potentiels de circulations des eaux souterraines de Mednine par imagerie satellitaire (Landsat). *1er congrès international : ISEE GEOMATICS. Tataouine*, 50-51.
- GennaA., LenôtreN. & Capdeville J.p.1997. Proposition d'un modèle d'inversion tectonique au Plio-Quaternaire dans les Corbières et le Minervois (France). Conséquences morphologiques et hydrologiques. *Comptes Rendus de l'Académie des Sciences - Series IIa - Earth and Planetary Science*, ,32, 10, 807-813. [https://doi.org/10.1016/S1251-8050\(97\)82760-7](https://doi.org/10.1016/S1251-8050(97)82760-7).
- Guellala R., Gannouni S., Khemiri R. et al. 2017.Une approche multidisciplinaire pour la recherche des ressources en eau dans un secteur touristique. Cas de la région de Tabarka (Nord-Ouest de la Tunisie). *La Houille Blanche*, 103, 1, 60-67. <https://doi.org/10.1051/lhb/2017009>.
- Guellala R., Tagorti M.A., Inoubli M.H. F et al. 2012 . Insights into Méjerda basin hydrogeology, Tunisia, *Applied Water Science journal*, 2, 3, 143–155. <https://doi.org/10.1007/s13201-012-0038-1>
- Gobashy M. M., Mekkawi M. M., Araffa S. A. S. et al. 2023. Magnetic Signature of Gold Deposits: Example from Um Garayat Region, South Eastern Desert, Egypt. *Pure and Applied Geophysics*, 180, 3, 1053-1080. <https://doi.org/10.1007/s11053-021-09897-3>.
- Ghassemi F. & Jakeman A. J. 2005. *Groundwater modelling in arid and semi-arid areas*. Cambridge University Press.
- Hoffmann J. & Sander P. 2007. Remote sensing and GIS in hydrogeology. *Hydrogeology Journal*, 15, 1-3. <https://doi.org/10.1007/s10040-006-0140-2>.
- Hezzi H. & Ghazouani L. 1996. *Compte Rendu de fin de travaux du forage Oued el Amor*. Rapport interne. Direction Générale des Ressources en Eau, 11p.
- Jauzein A. 1962. *Contribution à l'étude géologique des confins de la dorsale tunisienne*. Thèse de Doctorat en Sciences Naturelle, Université Paris, 475 p.
- Javhar A., Chen X., Bao A. et al. 2019. Comparison of Multi-Resolution Optical Landsat-8, Sentinel-2 and Radar Sentinel-1 Data for Automatic Lineament Extraction: A Case Study of Alichur Area. *Remote Sensing journal*, 11, 778. <https://doi.org/10.3390/rs11070778>.
- Jourda J. P., Saley M. B., Djagoua E. V. et al. 2006. Utilisation des données ETM+ de Landsat et d'un SIG pour l'évaluation du potentiel en eau souterraine dans le milieu fissuré précambrien de la région de Korhogo (nord de la Côte d'Ivoire) : approche par analyse multicritère et test de validation. *Télédétection journal*, 5, 4, 339-357.

- Kadri A. & Ben Haj Ali M. 1999. Eléments de réflexion sur les linéaments tectoniques Est-Ouest et Nord Sud et les grabens associés en Tunisie septentrionale, *Notes du Service Géologique de la Tunisie*, 65, 131-140.
- Kallali A., Ayadi R. & Manai K. 2006. *Compte Rendu de fin de travaux du forage de Tabarka 2*. Rapport interne. Direction Générale des Ressources en Eau, 5p.
- Kujawski J. 1964. Stratigraphie-Contribution à la connaissance stratigraphique de base de «flysch» oligocène de l'Extrême-Nord tunisien. *Comptes Rendus Hebdomadaires des Séances de l'Académie des Sciences*, 258, 1, 260-262.
- Kouamé K.F., Gioan P., Biémi J. et al. 1999. Méthode de cartographie des discontinuités-images satellitaires : Exemple de la région semi-montagneuse à l'ouest de la Côte d'Ivoire. *Télédétection*, 1, 139-156.
- Kouamé K.F., Akaffou A.G., Lasm T. et al. 2005. Simulation des écoulements dans les réservoirs fracturés : application au socle Archéen de Touba (Nord-Ouest de la Côte d'Ivoire). *Actes du Colloque Internationale SITIS 05, Yaoundé (Cameroun)*, 27 Nov.-1er Déc. (2005), 39-46.
- Laake A. 2011. Integration of satellite Imagery, Geology and geophysical Data. In I. A.Dar and M. A. Dar (Eds). *Earth and Environmental Sciences*, 467-492. <https://doi.org/10.5772/27613>.
- Larue J.P. 2005. Tectonique, érosion et hydrographie sur la bordure nord-ouest du Massif central (France). *Géomorphologie : relief, processus, environnement*, 11, 4, 275-296. <https://doi.org/10.4000/gemorphologie.499>.
- Lloyd J.W. 1999. Water resources of hard rock aquifers in arid and semi-arid zones. UNESCO, Paris. 281p.
- MacDonald A., Bonsor H.C., Dochartaigh B.E.O. et al. 2012. Quantitative maps of groundwater resources in Africa. *Environmental Research Letters*, 7, 2, 7p. <https://doi.org/10.1088/1748-9326/7/2/024009>.
- Mathew T.G., Ariffin K.S. 2018. Remote Sensing Technique for Lineament Extraction in Association with Mineralization Pattern in Central Belt Peninsular Malaysia. *Journal of Physics: Conference Series*, 1082, 6p. <https://doi.org/10.1088/1742-6596/1082/1/012092>
- Meijerink A.M.J., Bannert D., Batelaan,O. et al. 2007. *Remote sensing applications to groundwater*. UNESCO, Paris, 304p. <https://unesdoc.unesco.org/ark:/48223/pf0000156300>
- Mejri L. 2012. *Tectonique Quaternaire paléosismicité et sources sismogéniques en Tunisie (nord orientale) étude de la faille d'Utique*. Thèse de Doctorat, Université Toulouse 3 en cotutelle avec Université de Tunis el Manar, 193p.
- Moayedi H., Samani N. & Ebrahimi M. 2016. Geophysical investigation of alluvial aquifer geometry in the Karkheh River Basin, Iran. *Arabian Journal of Geosciences*, 9,7, 1-11.
- Nazih M., Gobashy M., Araffa S. et al. 2022. Geophysical studies to delineate groundwater aquifer in arid regions: A case study, Gara Oasis, Egypt. 2022. *Contributions to Geophysics and Geodesy*, 52, 4, 517-564. doi: 10.31577/congeo.2022.52.4.2
- O'leary D. W., Freidman J. D. & Pohn H. 1976. Lineament, linear, lineation: Some proposed new definitions for old terms. *Geological Society of America Bulletin*, 87, 10, 1463-1469. [https://doi.org/10.1130/0016-7606\(1976\)87<1463:LLLSPN>2.0.CO;2](https://doi.org/10.1130/0016-7606(1976)87<1463:LLLSPN>2.0.CO;2).
- Ould Bagga, M.A., Abdeljaouad, S. & Mercier, E., 2006. La “zone des nappes” de Tunisie : une marge méso-cénozoïque en blocs bascules modérément inverses (région de tabarka/Jendouba); Tunisie nord-occidentale). *Bull. Soc. Géol. Fr.*, (2006), 177, 145– 154.
- Ouertani N. 1978. *Compte Rendu de fin de travaux du forage de Tabarka*. Rapport interne. Direction Générale des Ressources en Eau , 5p.
- Paskoff R. & Sanlaville P. 1983. *Les côtes de la Tunisie. Variations du niveau marin depuis le Tyrrhénien*. Edition de la Maison de l'Orient et de la Méditerranée, 192p.
- PCI, Geomatica 2001. PCI Geomatica user 's guide version 9.1. Ontario. Canada. Richmond Hill.CD-ROM.
- Prost L.G. 2001. *Remote sensing for geologists: a guide to image interpretation*. New York:Marston., 702p.
- Rouvier H. 1977. Gitologie de l'extrême Nord du Tunisien : tectonique et paléogéographies superposées à l'extrémité orientale de la chaîne nord-maghrebine. *Annales des mines et de la géologie Tunisie*, 29, 427p.
- Rouvier H. & Ben Salem H. 1992. *Carte géologique 1/50 000 de Tabarka, Feuille n° 7*. Service géologique. Office National des Mines, Tunisie. <https://www.sudoc.fr/052015599>.
- Riahi S., Soussi M., Boukhalfa K., Ben Ismail L.K. et al. 2010. Stratigraphy, sedimentology and structure of ,the Numidian Flysch trust belt in northern Tunisia. *Journal of African Earth Sciences*, 57, 1-2,109–126. <https://doi.org/10.1016/j.jafrearsci.2009.07.016>.
- Roux J. & Harmand D. 1998. Contrôle morpho structural de l'histoire d'un réseau hydrographique : le site de capture de la Moselle. *Geodinamica Acta*, 11, 4, 149-162. <https://doi.org/10.1080/09853111.1998.11105316>.
- Sabins Jr. F. F. 1986. Remote sensing principles and interpretation. *Cartography*, 11, 4, 441p. <https://doi.org/10.1080/00690805.1980.10438124>.
- Salaj J., Batik P., Maameri N. et al. 1974. Le Sénonian supérieur et le Paléogène de la région des Hétil. Livret-guide des extrusions. VIème Colloque Africain de Micropaléontologie. *Edition de Service Géologique de Tunisie*, 59-66.
- Sghaier M., Trabelsi R. & Ben Dhia H. 2016. Sustainable water management in the Kairouan plain, central Tunisia, using a numerical model. *Hydrological Sciences Journal*, 61, 10, 1822-1836.
- Soesilo I. & Hoppin R.A. 1986. Evaluation of digitailly processed Landsat imagery and SIR-A imagery for plogical analysis of West Java region, Indonesia. *Symposium on Remote Sensing for Resources Development and Environmental Management*, 173- 182.

- Talbi F., Melki F., Ben Ismail L. K. et al. 2008. Le Numidien de la Tunisie septentrionale: données stratigraphiques et interprétation géodynamique. *Estudios Geológicos*, 64, 1, 31-44. <https://doi.org/10.3989/egeol.08641429>.
- Telford W. C., Geldard B.P. & Sheriff R. E. 1976. *Applied geophysics* (1st ed.). Cambridge University Press, 760p. <https://doi.org/10.1017/CBO9781139167932>.
- Yatabe S. & Howarth P.H. 1984. Lineament enhancement and interpretation in northern Ontario from airborne, multispectral scanner data. *Proceedings of the International Symposium on Remote Sensing, 3d Thematic conference, Remote Sensing for exploration Geology*, 1-8.
- Youan Ta. M. 2008. *Contribution de la télédétection et des systèmes d'informations géographiques à la prospection hydrogéologique du socle précamalien d'Afrique de l'Ouest : Cas de la région de Bondoukou Nord Est de la Côte d'Ivoire*. Thèse de doctorat, Université de Cocody-Abidjan, 236 p.
- Youan Ta. M., Lasm T., Jourda J.P. et al. 2008. Cartographie des accidents géologiques par imagerie satellitaire Landsat-7 ETM+ et analyse des réseaux de fractures du socle précamalien de la région de Bondoukou .*Télédétection*, 8 ,2, 119-135. <https://halshs.archives-ouvertes.fr/halshs-00392312>.

Manuscrit reçu le 30/10/2023
Version révisée acceptée le 24/05/2024
Version finale reçue le 18/10/2024
Mise en ligne le 28/10/2024